Dalton Transactions

Accepted Manuscript

This article can be cited before page numbers have been issued, to do this please use: R. Dorta, A. Ou, L. Wu, A. Salvador, G. Sipos, G. Zhao, B. W. Skelton and A. N. Sobolev, *Dalton Trans.*, 2017, DOI: 10.1039/C6DT04534K.

This is an Accepted Manuscript, which has been through the Royal Society of Chemistry peer review process and has been accepted for publication.

Accepted Manuscripts are published online shortly after acceptance, before technical editing, formatting and proof reading. Using this free service, authors can make their results available to the community, in citable form, before we publish the edited article. We will replace this Accepted Manuscript with the edited and formatted Advance Article as soon as it is available.

You can find more information about Accepted Manuscripts in the author guidelines.

Please note that technical editing may introduce minor changes to the text and/or graphics, which may alter content. The journal's standard Terms & Conditions and the ethical guidelines, outlined in our author and reviewer resource centre, still apply. In no event shall the Royal Society of Chemistry be held responsible for any errors or omissions in this Accepted Manuscript or any consequences arising from the use of any information it contains.

ROYAL SOCIETY OF CHEMISTRY

rsc.li/dalton

View Article Online
DOI: 10.1039/C6DT04534K

Journal Name

ARTICLE

New, Potentially Chelating NHC Ligands; Synthesis, Complexation Studies, and Preliminary Catalytic Evaluation

Received 00th January 20xx,
Accepted 00th January 20xx

DOI: 10.1039/x0xx00000x

www.rsc.org/

Arnold Ou,[a] Linglin Wu,[a] Alvaro Salvador,[a] Gellert Sipos,[a] Guangzhen Zhao,[a] Brian W. Skelton,[b] Alexandre N. Sobolev,[b] and Reto Dorta[a]

Abstract: Two new N-heterocyclic carbene (NHC) ligands bearing 2-morpholino and 2-piperidinyl naphthyl wingtips were synthesised (2-SIMorNap and 2-SIPipNap). Nuclear magnetic resonance studies, in conjunction with crystal structures and derivatisation of the NHC salts using a chiral counteranion, revealed that the ligand wingtips are oriented *anti* with respect to each other. From the free carbene, palladium, ruthenium and iridium complexes were prepared. NHC-iridium dicarbonyl complexes were made in order to extract the TEP values for these ligands. The study showed that these NHC ligands are more electron-donating than normal, aryl-substituted NHCs. The palladium complexes were tested in representative Suzuki-Miyaura cross-coupling reactions and compared to the state of the art systems. Ruthenium-catalysed ring-closing metathesis with these ligands was also performed. It was found that Grubbs' 2nd generation catalyst incorporating 2-SIPipNap did not initiate at room temperature and required heating for RCM to occur.

1. Introduction

The use of N-heterocyclic carbenes (NHCs) in transition metal catalysis had existed prior to the first isolation of a free NHC, and even then these ancillary ligands showed promise in the rhodium-catalysed hydrosilylation reactions.[1,2] Despite these encouraging early results, the use of NHCs in catalysis only became predominant after the isolation of a free NHC by Arduengo et al.,[3] and subsequent pioneering work of Herrmann and co-workers (Figure 1, right).[4]

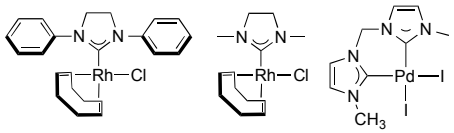

Figure 1: Early examples of NHC-metal complexes for catalysis

Following on from initial work of Herrmann and co-workers on the use of NHC-Ru complexes in olefin metathesis,[5] the groups of Grubbs,[6,7] and Nolan,[8] demonstrated that displacement of one phosphine ligand in Grubbs' catalyst with the NHC IMes or SIMes leads to catalyst systems that showed vastly improved behaviour. These results generated enormous interest and kick-started very successful developments within NHC-Ru metathesis that, inter alia, led to modifications of these NHC structures and more highly active and selective catalysts,[9,10] and most recently saw the development of highly Z-selective cross-metathesis catalysts by Grubbs et al..[11] In their report, NHCs bearing mixed aryl / adamantyl wingtips were used where the adamantyl group would undergo cyclometalation to generate a chelating NHC. Interestingly, C-H activation of the NHC ligand wingtips is in general proposed to be a major decomposition pathway for active species in NHC-Ru metathesis catalysts,[12] but in this case, opposite results were found.

The second major catalytic application where the power of such monodentate NHC ligands became evident early on saw the development of very active NHC-palladium catalysts for various cross-coupling reactions. Initially developed by Hermann and co-workers,[4] more recent results by the groups of Nolan,[13,14] and subsequently Organ,[15] have established NHC-palladium precatalysts with different labile or 'throw away' ligands [(substituted) allyl, substituted pyridine). These allow easy access to the catalytically active species and have pushed the boundaries in terms of possible cross-coupling reactions. Again and not unlike what has been developed in NHC-ruthenium chemistry, sterically demanding, monodentate NHCs with substituted aryl side chains have been the most successful designs in this application. Nevertheless, in these palladium-catalysed applications, the N-substituent in these monodentate NHC ligands can be varied more extensively as shown inter alia by Glorius and co-workers in his IBiox ligand family.[16,17]

Within our group, we have previously reported NHCs bearing 2-alkylnaphthyl and 2,7-alkylnaphthyl wingtips (Figure 2, left) and these were shown to be highly active in a range of palladium-catalysed cross-couplings and ruthenium-catalysed

[a] School of Chemistry and Biochemistry, University of Western Australia, 35 Stirling Highway, Perth 6009, Western Australia, Australia. Fax: (+61) 8 6488 7330; phone: (+61) 8 6488 3161; e-mail: reto.dorta@uwa.edu.au.
[b] Centre for Microscopy, Characterisation and Analysis, University of Western Australia, 35 Stirling Highway, Perth 6009, Western Australia, Australia.
Electronic Supplementary Information (ESI) available: [details of any supplementary information available should be included here]. See DOI: 10.1039/x0xx00000x

View Article Online
DOI: 10.1039/C6DT04534K

olefin metathesis reactions.[18] Enantiopure versions of these ligands were also developed and were found to perform well in α-arylations,[19] in the asymmetric Suzuki-Miyaura cross-coupling to give axially chiral biaryls,[20] and most recently in the asymmetric intramolecular hydroamination reaction.[18f] This latest contribution also highlighted the fact of the very likely involvement of a unique, transient second binding point in our NHC ligand family (reversible binding interaction of the metal with one of the naphthyl side chains), which would perfectly explain the overall often superior catalytic performance of our ligands when compared to the more classical IMes/SIMes and IPr/SIPr NHC ligand family.

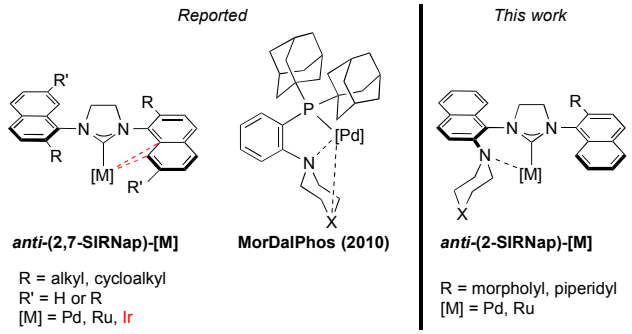

Figure 2: Reported (left, middle) and present (right) ligand designs

Extending from this work, we are now presenting new NHCs bearing tertiary cyclic amines on the naphthyl side chains, to give (a) potentially more direct and strong additional binding point(s), further aiding catalysis through stabilisation of reactive catalyst intermediates (Figure 2, right).[21] Direct inspiration for such a ligand design came from previous work by the group of Stradiotto et al., who had introduced the bulky phosphine ligand MorDalPhos (Figure 2, centre). This very successful ligand design was proposed to aid stabilisation of low-valent catalyst intermediates via both a κ^2-P,N binding mode as well as a κ^3-P,N,O binding mode.[22]

2. Results and Discussion

2.1 Synthesis and Characterisation of New NHC Ligands

The synthesis of the new ligands began with the preparation of the appropriately substituted naphthyl groups that serve as the wingtips of the NHC structure. This was achieved using a palladium-catalysed Buchwald-Hartwig amination between 2-bromonaphthalene and morpholine or piperidine, giving good to excellent yields of intermediate **1a** / **1b** (Scheme 1). This was followed by a regioselective bromination of the naphthalene at the 1-position, where bromination with Br_2 was carried out at low temperature to give high yields of **2a** / **2b**. The ethylenediamine-based backbone of the NHC was then installed with a double Buchwald-Hartwig amination, giving diamines **3a** / **3b** in good to excellent yields after purification. Finally, ring-closure with triethyl orthoformate led to the formation of the NHC salts 2-SIMorNap•HBF_4 (**4a**) and 2-SIPipNap•HBF_4 (**4b**) (Mor = morpholyl; Pip = piperidyl).

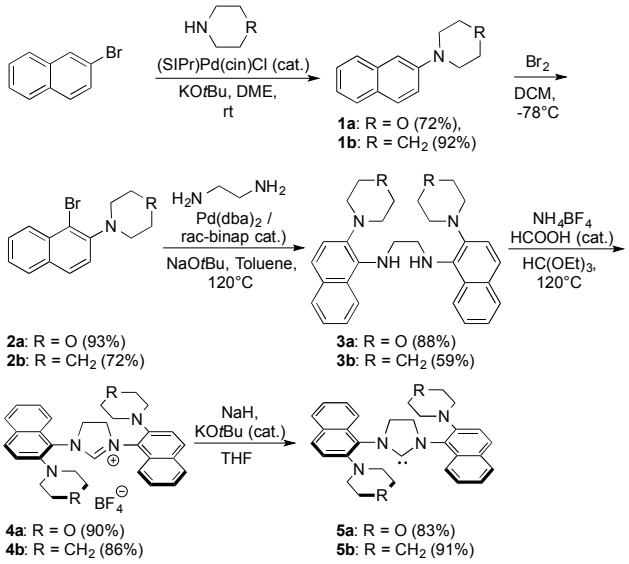

Scheme 1: Synthetic pathway to bis(2-aminonaphth-1-yl)-N-heterocyclic carbene ligands 2-SIMorNap (**5a**) and 2-SIPipNap (**5b**).

Interestingly, we found that our new NHC salts are ring-closed to give what appeared to be the *anti*-configured naphthyl wingtip isomers exclusively. For instance, variable temperature ^{1}H NMR spectroscopy of 2-SIMorNap•HBF_4 (**4a**) from 25°C to -60°C (acetone-d_6) revealed no signal splitting of the N-C**H**-N proton (see the supporting information) with a negligible second signal further downfield becoming apparent at lower temperatures (see Supporting Information, <2%). The signal pattern at around 5 ppm, which corresponds to the backbone $(CH_2)_2$ group of the N-heterocycle, also suggested the absence of a *syn*/*anti* mixture of isomers. This result is in stark contrast to our group's past reports, where a diverse array of NHC salts bearing 2-alkylnaphthyl and 2,7-dialkylnaphthyl wingtips would invariably show two sets of signals for the imidazolinium proton, corresponding to the two possible orientations of the naphthyls with respect to each other, namely *syn* or *anti*.[18,23] At least at the salt stage, interconversion of these NHC isomers is not observed,[18a] and the ratio would vary according to the bulk introduced, with sterically more demanding and cyclic alkyl groups heavily favouring the *anti*-isomer. For example and as a sterically very similar imidazolinium salt to **4a** and **4b**, the cyclohexyl-substituted 2-SICyNap•HBF_4 (Cy = cyclohexyl) shows an approximately 3:1 *anti*:*syn* ratio. The most likely cause for the *anti*-isomer to prevail in **4a** and **4b** is electrostatic, where a *syn*-arrangement of the naphthyl side chains would result in repulsion between the two approaching nitrogen atoms of the morpholyl and piperidyl substituents, thus rendering generation of the *syn*-isomer during ring-closing unfavourable.

Not surprisingly then, when single crystals of 2-SIMorNap•HBF_4 (**4a**) and 2-SIPipNap•HBF_4 (**4b**) were grown and subjected to X-ray diffraction analyses, they confirmed the expected C_2-symmetric *anti*-isomer in the solid state (Figure 3).[24] The NCCN backbones of the N-heterocycle in both NHC

View Article Online
DOI: 10.1039/C6DT04534K

salts were found to be significantly twisted with torsion angles of 19.7(2)° for NHC salt **4a** and 17.8(1)° for **4b**. These values are clearly higher when compared to our previously reported, very similar NHC salt 2-SICyNap•HBF_4, in which the backbone torsion angle is much lower (5.18°).[18b]

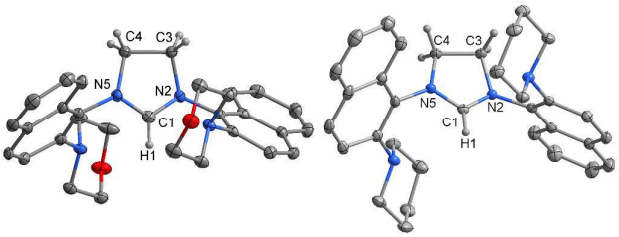

Figure 3: Diagrams of the cation of the NHC salts 2-SIMorNap•HBF_4 (**4a**) (left) and 2-SPipNap•HBF_4 (**4b**) (right) with ellipsoids drawn at the 50% probability level. Hydrogen atoms, except for those on the N-heterocyclic ring, have been omitted for clarity. Selected bond angles [°] **4a**: N5-C1-N2 115.0(2), N5-C4-C3-N2 19.7(2)˚. **4b**: N5-C1-N2 114.7(1), N5-C4-C3-N2 17.8(1)˚.

Deprotonation of the imidazolinium salts (**4a** and **4b**) led to clean formation of free NHCs **5a** and **5b**, as confirmed by ^{1}H NMR (loss of the N-C*H*-N signal) and by $^{13}C\{^1H\}$ NMR spectroscopy, with the appearance of a single singlet for the characteristic downfield carbene signal (≈246 ppm). This value falls within the narrow range seen for our previously reported structures. Another very diagnostic signal (single doublet) is attributed to the H^8 protons of the naphthyl units in the ^{1}H NMR spectrum. That a single signal is detected for both the carbene and the H^8 protons in fact means that even at the deprotonated stage, structures **5a** and **5b** exist as their *anti*-isomers only. This is in contrast to e.g. (2)-SIMeNap, where deprotonation leads to a situation where the naphthyl side chains are able to freely rotate.[18a] Crystal structures of both these free carbenes (**5a** and **5b**) were also obtained and as expected, the structures again showed the *anti*-configuration as represented in Figure 4.[24] Upon going from the imidazolinium salts **4a**/**4b** to the free N-heterocyclic carbenes **5a**/**5b**, we can see the relief of strain in the backbone of the N-heterocycle with the torsion angles being reduced to 10.8(3), 10.2(2)˚ (**5a,** molecule 1 and 2) and 9.2(1)° (**5b**). The N2-C1-N5 angles follow a similar trend and widen significantly upon deprotonation and generation of the free carbenes **5a**/**5b**. The values of these angles are, somewhat not surprisingly, substantially larger when compared to unsaturated NHCs with similar steric bulk such as IMes or IPr.[25] It should be noted here that X-ray crystallographic analyses of such imidazolin-2-ylidene structures are still rare. Indeed, only SIMes,[26] SI^{t}Bu,[27] and SIPr,[28] have been reported besides our previously reported naphthyl-based NHCs. Even rarer are structures such as **5a** / **5b** that feature additional functional groups on the wingtips, with the only other structure we are aware of (featuring an imine group within one of its side chains) reported in 2014.[29]

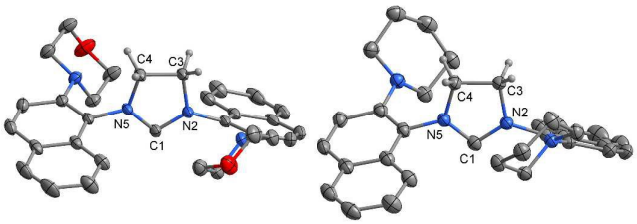

Figure 4: Diagrams of the NHCs 2-SIMorNap **5a** (left, molecule 1) and 2-SIPipNap **5b** (right) with ellipsoids drawn at the 50% probability level. Hydrogen atoms except, for those on the N-heterocyclic, have been omitted for clarity. Selected bond angles and torsion angles [°] **5a**: N5-C1-N2 104.9(1), N7-C6-N10 104.9(1)˚, N5-C4-C3-N2 9.7(1), N7-C8-C9-N10 10.3(1)˚. **5b**: N5-C1-N2 105.5 (1), N5-C4-C3-N2 9.2 (1)˚.

Because of the fact that *anti*-(2-SIMorNap)•HBF_4 (**4a**) and *anti*-(2-SIPipNap)•HBF_4 (**4b**) present C_2-symmetric structures and knowing that conversion to the *syn* isomers is not occurring in these salts,[18a] we reckoned that the two possible atropisomers might be spectroscopically distinguishable when generating the corresponding diastereoisomers after an anion exchange with silver (*S*)-camphorsulfonate. In the ideal case and with a solvent that maintains a tight ion pair in these salts, two separate signals for the imidazolinium proton (C1-H) of each of the atropisomers [(R_a,R_a,*S*) or (S_a,S_a,*S*)] would be observable [three signals in total if the *syn*-isomer is present (achiral *meso* compound)]. To confirm this, we prepared NHC•HCl salts **4c** and **4d**, that were then subjected to salt metathesis using silver (*S*)-camphorsulfonate to generate the corresponding NHC•H[(*S*)-camphorsulfonate] salts **4c*** and **4d*** (Scheme 2). When **4c*** was analysed by ^{1}H NMR spectroscopy (CD_2Cl_2) at room temperature, the signal for the C1-H proton appeared as a broad singlet. Gradually lowering the temperature then led to the expected splitting (1:1 ratio) for the imidazolinium proton below -20°C as shown in Figure 5.[30] With **4d*** on the other hand, splitting of the C1-H proton began at -5°C and by -20°C, complete separation into two individual singlet signals was observed in the expected 1:1 ratio corresponding to the (R_a,R_a,*S*)-**4d*** and (S_a,S_a,*S*)-**4d*** isomers (Figure 6). This experiment clearly confirmed the assignment for species **4** as being the *anti* isomer and might offer a method for separating these racemic compounds.[31]

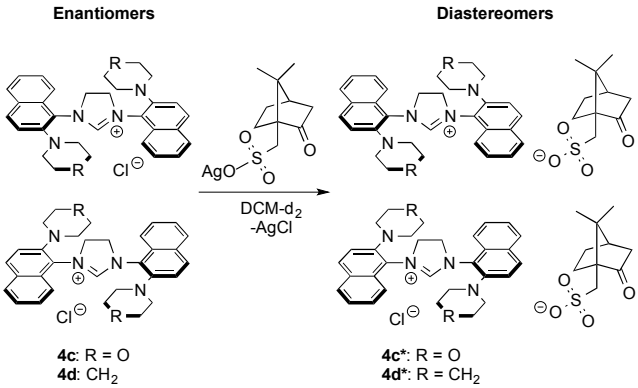

Scheme 2: Anion exchange between NHC•HCl and silver (*S*)-camphorsulfonate.

View Article Online
DOI: 10.1039/C6DT04534K

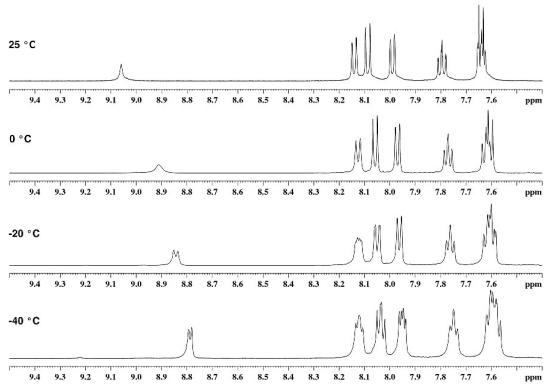

Figure 5: Stacked ^{1}H NMR spectra (CD_2Cl_2) of **4c*** at various temperatures.

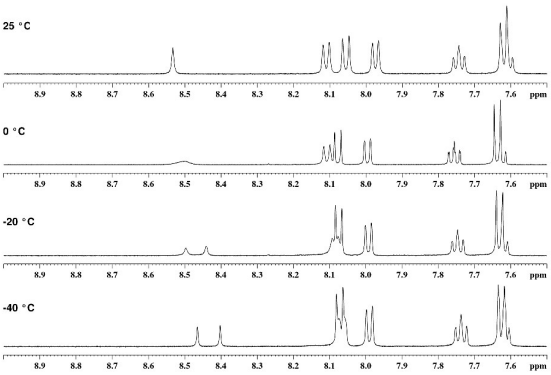

Figure 6: Stacked ^{1}H NMR spectra (CD_2Cl_2) of **4d*** at various temperatures.

2.2 Synthesis and Characterisation of New NHC Complexes

With the two new ligands **4a**/**5a** and **4b**/**5b** in hand, we next proceeded to synthesise catalytically relevant palladium and ruthenium complexes containing them. Palladium complexes (**6a** and **6b**) were prepared by mixing the respective free NHCs **5a** and **5b** with $[Pd(cin)Cl]_2$ (cin = cinnamyl) in THF (Scheme 3, top). The ensuing palladium complexes **6a** and **6b** were purified by passage through a short silica gel column and subsequent crystallisation. As shown in Figure 7, crystal structures of the palladium complexes reveal a distorted square planar geometry for both **6a** and **6b**.[24] Not surprisingly, the naphthyl side chains are arranged *anti* with respect to each other. The cinnamyl ligand was found to be distorted around the palladium, a phenomenon that was also evident in solution (^{1}H NMR spectroscopy), where the signals corresponding to the cinnamyl moieties appear as broadened entities. Complexes [(2-SIMorNap)Pd(cin)Cl] (**6a**) and [(2-SIPipNap)Pd(cin)Cl] (**6b**) have NHC-Pd bond lengths of 2.037(2)Å (**6a**) and 2.047(7), 2.058(7) Å (molecules 1,2 of **6b**), values which fall within the range of reported bond lengths of NHC-Pd complexes of this type.[13,14,18e,32] Palladium-cinnamyl bond lengths between the two complexes were also noticeable, with **6a** having longer bond lengths compared to **6b**. It has been suggested that the bond lengths between the allyl and the palladium is an indicator of the complexes' ease of activation, with a longer bond length implying that the necessary generation of the catalytically active NHC-Pd(0) species is more facile.[14]

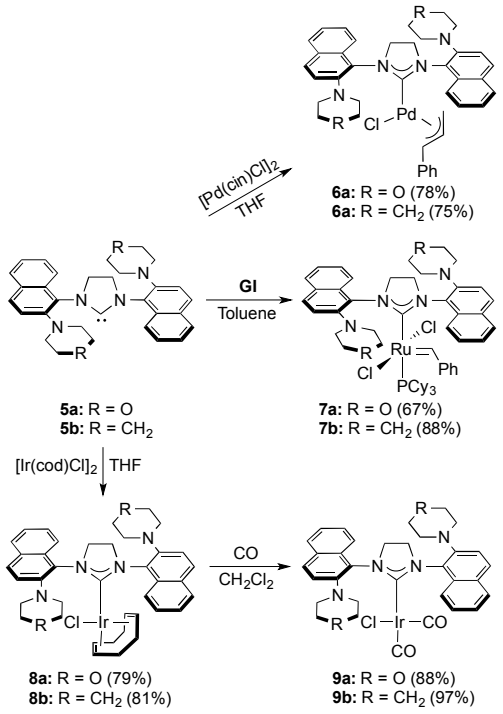

Scheme 3: Synthetic access to NHC-Pd, NHC-Ru and NHC-Ir complexes.

We then moved to the synthesis of derivatives of second-generation Grubbs-type precatalysts (**GII**) incorporating our new NHC ligands. These compounds were prepared by the displacement of one tricyclohexylphosphine with **5a**/**5b** on the first generation Grubbs catalyst (**GI**, Scheme 3, middle) in toluene. Filtration over Celite® the next day and subsequent removal of the solvent led to the desired complexes **7a** and **7b** respectively, which were further cleaned by repeated washing with n-pentane. NMR spectroscopic data again clearly indicated the presence of the *anti*-isomer species of the NHC ligands, with the $^{31}P\{^{1}H\}$ NMR spectrum giving a single signal and ^{1}H and $^{13}C\{^{1}H\}$ NMR spectra all but confirming the absence of a *syn*/*anti* mixture of the possible NHC isomers. The benzylidene C-H signal was located at the expected low-field region at 19.26 (**7a**) and 19.69 (**7b**) ppm respectively. In the $^{13}C\{^{1}H\}$ NMR spectrum, the benzylidene carbon signal was found at 297.05 ppm (**7a**) and 297.65 ppm (**7b**), with the NHC carbene as expected more upfield with respect to these (222.27 and 221.93 ppm).

View Article Online
DOI: 10.1039/C6DT04534K

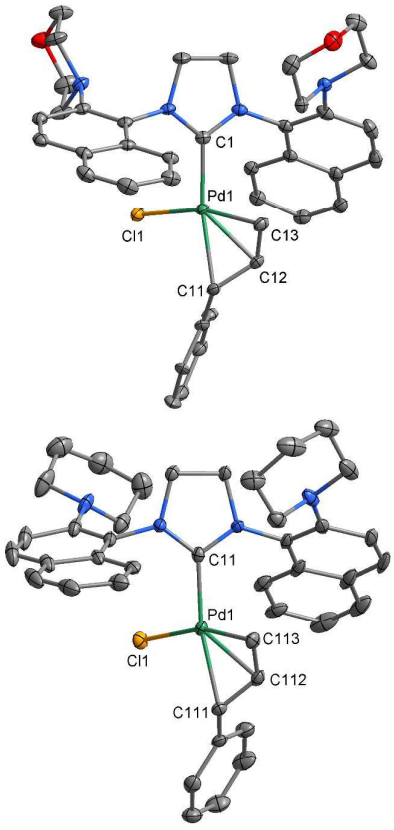

Figure 7: Diagrams of **6a** (upper) and **6b** (lower, molecule 1) with ellipsoids drawn at 30% probability level and with hydrogen atoms omitted for clarity. Selected bond lengths [Å]: **6a**: C1-Pd1 2.037(2), C13-Pd1 2.110(2), C12-Pd 2.166(5), C11-Pd1 2.311(4)Å. **6b**: C11-Pd1 2.047(6), C113-Pd1 2.102(7), C112-Pd1 2.140(7), C111-Pd1 2.273(7), C21-Pd2 2.058(7), C213-Pd2 2.125(7), C212-Pd2 2.141(7), C211-Pd2 2.251(6)Å.

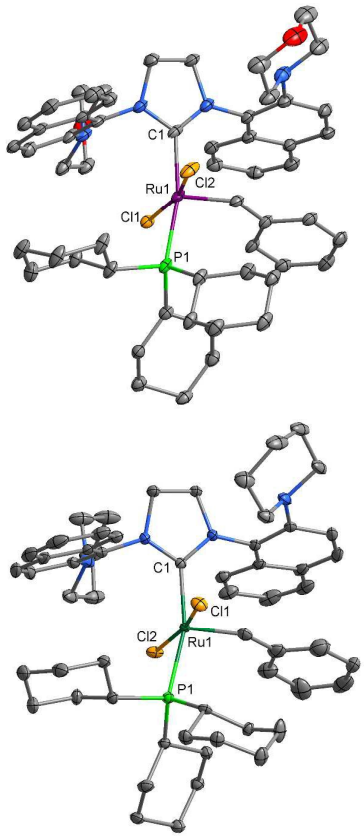

Figure 8: Diagrams of **7a** (upper, molecule 1 only shown) and **7b** (lower) with ellipsoids drawn at the 30% probability level and with hydrogens omitted. Selected bond lengths [Å] and angles [°]: **7a**: C1-Ru1 2.097(6), P1-Ru1 2.441(2), C200-Ru1 1.842(6), Cl1-Ru1 2.369(1), Cl2-Ru1 2.397(1)Å; Cl1-Ru1-Cl2 164.97(6), C1-Ru1-P1 165.4(2)°. C6-Ru2 2.100(6), P2-Ru2 2.437(2), C440-Ru2 1.826(6), Cl3-Ru2 2.371(1), Cl4-Ru2 2.401(1)Å; Cl3-Ru2-Cl4 165.06(6), C6-Ru2-P2 166.8(2)° **7b**: C1-Ru1 2.086(3), P1-Ru1 2.4371(9), C100-Ru1 1.819(9), Cl1-Ru1 2.3882(9), Cl2-Ru1 2.3822(9)Å; Cl1-Ru1-Cl2 167.84(4), C1-Ru-P1 162.4(1)°.

Full characterisation of complexes **7a** and **7b** again included structural determination via X-ray crystallographic analyses of crystals grown from layering pentane on top of concentrated dichloromethane solutions containing the compounds.[24] The structures of **7a** and **7b** are depicted in Figure 8 and key bond lengths and angles are given in the caption. Both complexes have a distorted square pyramidal geometry, in line with such **GII** (and **GI**) type complexes. Complexes **7a** and **7b** are overall very similar to the NHC-Ru complexes we have previously reported,[18c,d] and to the X-ray structures reported for the **GII** complex that features the parent SIMes ligand.[33] As can be seen, both NHC ligands are again *anti*-configured in complexes **7a** and **7b**. NHC-Ru bond lengths were found to be 2.097(6) Å and 2.100(6) Å for (2-SIMorNap)$RuCl_2$(=CHPh)(PCy_3) (**7a**) and 2.086(3) Å for (2-SIPipNap)$RuCl_2$(=CHPh)(PCy_3) (**7b**). Ru=C(benzylidene) bond lengths as well as the Ru-PCy_3 bond distances were also in line with values measured in such complexes as were the most important bond angles around the metal centre [Cl-Ru-Cl and P-Ru-C(NHC)].

Finally, we also wanted to synthesise NHC-iridium complexes containing our two new ligands, as carbonyl-containing iridium species would give us an indirect means to evaluate and compare electronic aspects of our ligands through measuring the π-donating ability of the metal centre. Therefore, NHC-iridium compounds containing 1,5-cyclooctadiene (cod) were synthesised by adding free NHCs **5a** or **5b** to a solution of $[Ir(cod)Cl]_2$ in THF (Scheme 3, bottom left). Stirring for two hours gave a yellow suspension from which the solvent was removed, the respective complexes then redissolved in dichloromethane (DCM) and filtered. Removal of the dichloromethane and final washings with pentane led to the desired complexes [(2-SIMorNap)Ir(cod)Cl] (**8a**) and [(2-SIPipNap)Ir(cod)Cl] (**8b**). These compounds were then used to access the relevant iridium-carbonyl complexes via bubbling of carbon monoxide through a solution of **8a** and **8b** in DCM (Scheme 3, bottom right). This led to displacement of the cod ligand and the formation of the iridium carbonyl complexes *cis*-[(2-SIMorNap)$Ir(CO)_2Cl$] (**9a**) and *cis*-[(2-SIPipNap)$Ir(CO)_2Cl$] (**9b**) after appropriate workup.

View Article Online
DOI: 10.1039/C6DT04534K

Crystal structures of these new iridium complexes were obtained,[24] with the exception of [(2-SIPipNap)Ir(cod)Cl] (**8b**), where multiple attempts invariably gave crystals of poor quality. In all of these structures, the NHC ligand again adopts the C_2-symmetric *anti*-orientation of its naphthyl wingtips, with the two morpholine / piperidine groups oriented away from each other. The NHC-Ir (C1-Ir1) bond lengths of **8a** are 2.072(6) and 2.055(6) Å for the two independent molecules. (Molecule 1 is shown in Figure 9). These values are slightly longer than reported values of complexes incorporating saturated NHCs SIPr and SIMes {[(SIPr)Ir(cod)Cl]; 2.049(5) Å: [(SIMes)Ir(cod)Cl]; 2.041(3) Å},[34a] and clearly longer when compared to our recently reported [(*anti*-2-SICyNap)Ir(cod)Cl] complex [2.034(1)].[18f] A comparison of the bond lengths of the olefin moieties reveals that they follow the expected trend with Ir-olefin distances distinctly longer for the fragment residing trans to the NHC as compared to the olefin trans to the chloride ligand, underlining the fact that the NHC ligand exhibits a higher trans influence than the chloride.

NHC-iridium carbonyl complexes *cis*-[(2-SIMorNap)Ir(CO)$_2$Cl] (**9a**) and *cis*-[(2-SIPipNap)Ir(CO)$_2$Cl] (**9b**) were crystallised and were found to be disordered with the carbonyl ligand (*cis* to the NHC) and the chloride ligand occupying the same position (rotational disorder). C1-Ir1 bond lengths were found to be 2.077(2) Å and 2.094(3) Å for **9a** and **9b**, respectively (Figure 10). These values are in line with reported values for the parent *cis*-[(SIPr)Ir(CO)$_2$Cl] (2.071(4) Å) and *cis*-[(SIMes)Ir(CO)$_2$Cl] (2.121(4) Å).[32] The overall geometries for both the Ir-cod complex **8a** and Ir-CO compounds **9a** and **9b**, show that they are almost perfectly square planar with the expected bond angles deviating only marginally from the idealised case. Because the cod ligand and the NHC in complex **8a** create a sterically rather crowded situation, we see a slight opening of the NHC-Ir-cod(olefin) angle to better accommodate the protruding naphthyl side chains sitting above C111-C112. Indeed, the hydrogen atoms on these olefinic carbons seem to interact with the aromatic moiety via σ-π interactions [H112···C(centroid) 2.56Å in molecule 1 and H216···C(centroid) 2.65Å in molecule 2]. Also noteworthy is the fact that the cod group in **8a** appears to be further locked into place by the chloride ion, with Cl-H(olefin) distances at around 2.6 Å.

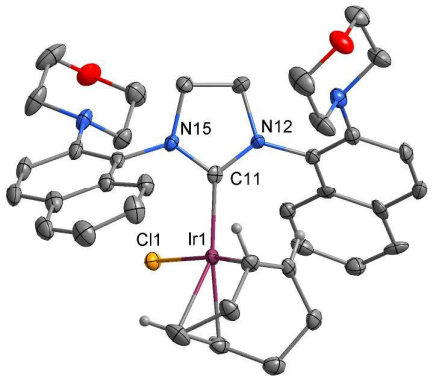

Figure 9: Diagram of **8a** (one of two independent molecules shown) with ellipsoids drawn at the 50% probability level and with hydrogens omitted. Selected bond lengths [Å] and angles [°]: **8a**: C11-Ir1 2.072(6), C111-Ir1 2.135(6), C112-Ir1 2.102(6), C115-Ir1 2.205(6), C116-Ir1 2.165(6), Cl1-Ir1 2.371(2)Å; C11-Ir1-Cl1 90.73(15), C11-Ir1-C111 96.7 (2), C11-Ir1-C112 97.2(2), C115-Ir1-Cl1 86.93(17), C116-Ir1-Cl1 87.45(18)˚. C21-Ir2 2.055(6), C211-Ir2 2.195(6), C212-Ir2 2.169(6), C215-Ir2 2.125(6), C216-Ir2 2.100(6)Å, Cl2-Ir2 2.369(2); C21-Ir2-Cl2 90.54(17), C21-Ir2-C215 96.3(2), C21-Ir2-C216 95.7(2), C211-Ir2-Cl2 87.89(18), C212-Ir2-Cl2 86.79(18)˚.

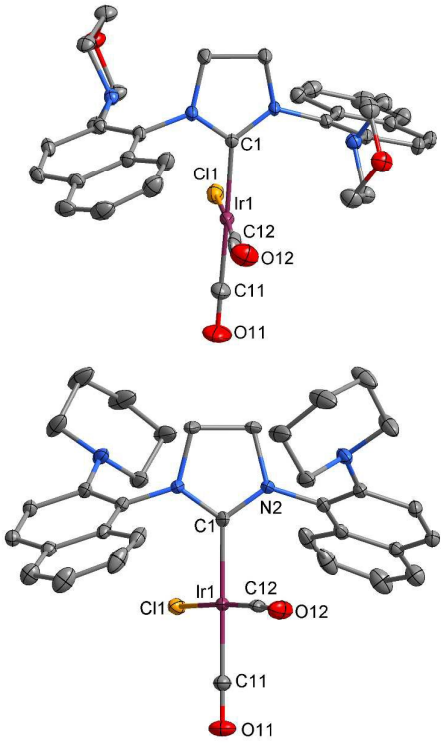

Figure 10: Diagrams of **9a** (upper) and **9b** (below) with ellipsoids drawn at the 50% probability level and with hydrogens omitted. Selected bond lengths [Å] and angles [°]: **9a**: C1-Ir1 2.077(2), Ir1-Cl1 2.287(1), C11-Ir1 1.897(3), C12-Ir1 1.936(6)Å; C11-Ir1-Cl1 87.73(11), C12-Ir1-C1 92.1(2)˚. **9b**: C1-Ir1 2.094(3), Ir1-Cl1 2.377(2), C11-Ir1 1.912(4), C12-Ir1 1.792(8)Å; C11-Ir1-Cl1 88.7(4), C12-Ir1-C1 91.5(2)˚.

2.3 Comparison of the electronic properties of NHC's 5a and 5b

Infrared spectroscopy of complexes **9a** and **9b** showed two stretching bands for the carbonyl ligands. Averaged values of these two carbonyl signals were then used to calculate the Tolman electronic parameter (TEP).[33b,34] For the *cis*-[(2-

View Article Online
DOI: 10.1039/C6DT04534K

SIMorNap)Ir(CO)$_2$Cl] (**9a**) complex, a TEP value of 2050 cm^{-1} was found using Nolan's modified correlation between such iridium systems and the original nickel carbonyl compounds. The value implies that the NHC ligand **5a** is slightly more electron-donating than our analogous, previously reported 2-cyclohexyl substituted 2-SICyNap ligand.[18b] A further decrease in the TEP value is seen in 2-SIPipNap (**5b**). Within saturated NHCs with a non-modified five-membered N-heterocycle, **5b** is indeed at the very low end of the TEP values recorded so far.[33b] That said and as pointed out in the past, the TEP values of NHC structures such as the ones shown in Table 1 are overall very similar. In fact, the only way to decidedly change the electronics of these species is to introduce pertinent variations to the five-membered N-heterocycle itself, by e.g. substituting and electronically altering the backbone positions.[34b,35b]

Table 1: List of average CO stretching frequencies and TEP values of selected NHCs.[a]

Ligand	Solvent	ν_{CO}^{av} (cm^{-1})	TEP (cm^{-1})
SIPr[b]	CH_2Cl_2	2024.9	2051.1
SIMes[b]	CH_2Cl_2	2024.6	2050.8
IPr[b]	CH_2Cl_2	2023.9	2050.2
IMes[b]	CH_2Cl_2	2023.1	2049.6
ICy[b]	CH_2Cl_2	2023.0	2049.5
IAd[b]	CH_2Cl_2	2021.6	2048.3
2-SICyNap[c]	CH_2Cl_2	2025	2051
2,7-SICyNap[c]	CH_2Cl_2	2024	2050
2-SIMorNap[a]	CH_2Cl_2	2024	**2050**
2-SIPipNap[a]	CH_2Cl_2	2023	**2049**

[a]Calculated from the formula: TEP = 0.847 ν_{CO}^{av} + 336
[b]Taken from reference 33b. [c]Taken from reference 18f, decimal point omitted.

2.3 Catalytic Evaluation of the NHC-Pd and NHC-Ru Complexes

With the NHC-Pd and NHC-Ru complexes in hand, we next proceeded to evaluate their performance in typical benchmark reactions.

We began our investigation with the palladium complexes [(2-SIMorNap)Pd(cin)Cl] (**6a**) and [(2-SIPipNap)Pd(cin)Cl] (**6b**) and focused on the Suzuki-Miyaura cross-coupling reaction. Conditions that were used (Table 2) were similar to the ones we have reported before for the Suzuki-Miyaura coupling generating tetra-*ortho*-substituted biaryl products,[18e] where the same precatalyst, but incorporating an NHC with 2,7-cyclooctyl disubstituted naphthalene wingtips, was used to couple these challenging substrates at room temperature.

The first two entries in Table 2 show that the cross-coupling of bromobenzene and 4-toylboronic acid, with a relatively high catalyst loading (5 mol% of **6a** or **6b**), led to the desired product in high isolated yields at room temperature. Since the complexes performed well in this first benchmark reaction, we decided to use a more hindered substrate (2-bromotoluene and naphthylboronic acid), where we already saw an attenuated reactivity with lower isolated yields (Table 2, entries 3,4). The cross-coupling between chlorobenzene and 3-toylboronic acid (entries 5,6) also led to reasonable yields, where we also saw a clear difference of reactivity between the two catalysts with [(2-SIPipNap)Pd(cin)Cl] (**6b**) outperforming **6a**.

Table 2: Suzuki-Miyaura cross-coupling reaction using precatalysts **6a** and **6b**.

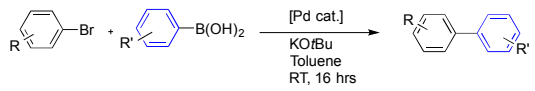

Entries[a]	Ar-X	Ar'-B(OH)$_2$	Ar-Ar'	cat. (mol%)	Yield[b]
1		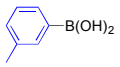	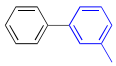	**6a** (5 mol%)	95%
2				**6b** (5 mol%)	92%
3		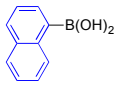	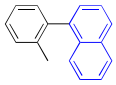	**6a** (5 mol%)	73%
4				**6b** (5 mol%)	74%
5		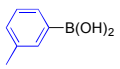	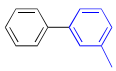	**6a** (5 mol%)	81%
6				**6b** (5 mol%)	93%
7		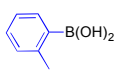	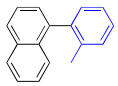	**6b** (5 mol%)	n.r
8	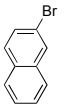	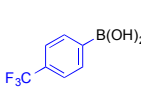	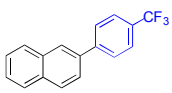	**6b** (5 mol%)	49%
9		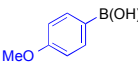	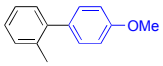	**6a** (5 mol%)	n.r
10		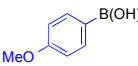	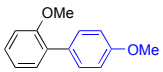	**6a** (5 mol%)	n.r
11	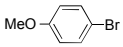	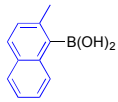	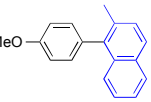	**6a** (5 mol%)	n.r
12		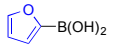	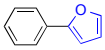	**6a** (5 mol%)	n.r
				6b (5 mol%)	n.r
13		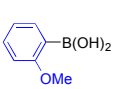	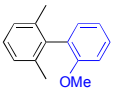	**6a** (5 mol%)	n.r
				6b (5 mol%)	n.r
14	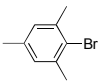	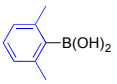	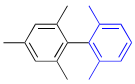	**6a** (5 mol%)	n.r
				6b (5 mol%)	n.r

Reaction conditions: Aryl bromide (0.4 mmol), aryl boronic acid (0.6 mmol), KO*t*Bu (1.0 mmol), Toluene (2 mL), RT and catalyst (5 mol%). [a] aryl boronic acid (0.8 mmol). [b]Isolated yields. nr = no reaction.

Unfortunately, both catalysts performed rather poorly with other coupling partners under these reaction conditions. Already modifying the electronic properties of the arylboronic acid completely inhibited product formation under room temperature conditions (entries 8-10, 12). Increasing bulk by placing groups at the *ortho* position of the arylboronic acid was also detrimental and did not show any generation of the coupled product (entry 7). Not surprisingly, increasing the bulk on the substrates even further (entries 13,14) did also not give any product under these mild reaction conditions. While earlier results in our group had shown that slight modifications

View Article Online
DOI: 10.1039/C6DT04534K

of these naphthyl-based NHC ligands does profoundly influence the reactivity of these [(NHC)Pd(cin)Cl] precatalyst,[18a,b,e] we nevertheless did not expect the results recorded here. Any explanation as to why these new ligands do not perform well in the Suzuki-Miyaura reaction is speculative, but it is reasonable to assume that it involves the potentially binding nitrogen atoms in the morpholine/piperidine units that are attached to these NHC ligands and that hamper efficient turnover at some point in the catalytic cycle.[36]

We then turned our attention to the catalytic evaluation of ruthenium complexes (2-SIMorNap)$RuCl_2$(=CHPh)(PCy_3) (**7a**) and (2-SIPipNap)$RuCl_2$(=CHPh)(PCy_3) (**7b**). For this, we chose a select few benchmark substrates for the ring-closing metathesis (RCM) reaction. Here again, we had shown earlier that NHCs with 2- or 2,7-alkyl substituted naphthyl side chains perform well in these and related cross metathesis (CM) reactions.[18c,d] We first tried to perform the ring-closing metathesis reaction with diethyl diallylmalonate (DEDAM) in the presence of **7a** or **7b** (1 mol%), directly following the conversion by running the reaction in dichloromethane-d_2 at room temperature. The experimental setup chosen here was identical to the one that our group had reported before for other **GII** analogues, including (2-SICyNap)$RuCl_2$(=CHPh)(PCy_3), a ligand that incorporates a cyclohexyl instead of a morpholine/piperidine unit on its naphthyl wingtips (see discussion above). To our surprise, the reactivity of these new catalysts was very poor, giving less than 10% conversion even after a prolonged reaction time in dichloromethane-d_2 at room temperature. For comparison, complete conversion within 20 minutes was observed for (2-SICyNap)-**GII**.[37] To understand whether this lack of reactivity was due to a slow initiation step of the catalyst,[38] we switched to toluene as a solvent and performed the same reaction under heating (60°C). Gratifyingly, with heating (60°C, toluene-d_8), the ring-closing metathesis of DEDAM proceeded with both **7a** and **7b**. While **7a** seemed to initiate quicker, the conversion of starting material to product stopped at approximately 50%, due to what appears to be relatively fast and irreversible catalyst decomposition. **7b** fared better and reached approximately 65% conversion in this first try (no internal standard).

With this knowledge and these reaction conditions in place, we performed a set of test reactions employing **7b**. The yield of the ring-closing metathesis reaction with DEDAM was 62% (1 mol% **7b**) based on ^{1}H NMR spectra with an internal standard (Table 3, entry 1). Ring-closure of linalool with **7b** (1 mol%) gave full conversion and a 97% yield as determined by ^{1}H NMR spectroscopy with an internal standard (Table 3, entry 2). The ring-closure of diallyl tosylamide was also successful and the product was isolated in 81% isolated yield (Table 3, entry 3). It should be noted that this result is in line with previous studies, which showed that RCM of the tosylamide substrate is somewhat more facile that the DEDAM reaction. Finally, enyne metathesis of (1-(allyloxy)prop-2-yne-1,1-diyl)dibenzene (Table 3, entry 4) also proceeded smoothly under these reaction conditions giving an isolated yield of the corresponding diene of 95%. Overall though and not unlike what we have seen above for the Suzuki-Miyaura coupling with palladium (pre)catalysts **6a**/**6b**, the reactivity of **7b** (and **7a**) is greatly attenuated compared to our previously reported alkyl-substituted members of these naphthyl-wingtipped **GII** analogues.

Table 3: Ring-closing reactions using precatalyst **7b**.

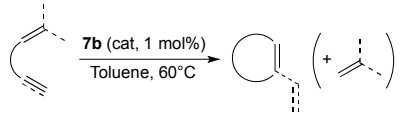

Entries	Substrate	Product	Yield
1[a]	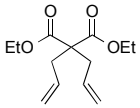	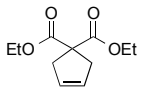	62%[c]
2[a]	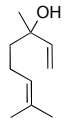		97%[c]
3[b]			81%[d]
4[b]	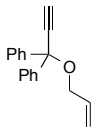		95%[d]

[a]Substrate (0.1 mmol), **7b** (1 mol%), Toluene (1.0 mL), 15 minutes, 60°C. [b]Substrate (0.5 mmol), **7b** (1 mol%), Toluene (5.0 mL), 15 minutes, 60°C. [c]Yield determined by NMR with an internal standard [1,2,3-trimethoxybenzene (0.1 mmol)]. [d]Isolated yield.

3. Conclusions

In conclusion, we have prepared two new N-heterocyclic carbene ligands with 2-morpholino-naphthyl and 2-piperidinyl-naphthyl wingtips. The idea behind the synthesis of these ligands came from recent studies on related ligand structures where the potential for having a second coordination site (hemilability) leads to increased catalytic behaviour. Access to both the NHC salts and the free carbenes of these new ligands was straightforward. Contrary to their 2-alkylnaphthyl analogues, these new ligands were produced with their two naphthyl sidechains arranged *anti* with respect to each other, both in the salt and the free carbene. Indeed and to unambiguously confirm it, we generated diastereomers of their salts by simply exchanging the anion with (*S*)-camphorsulfonate. Subsequent NMR studies showed the expected splitting of the imidazolinium proton for these diastereomeric ion pairs.

New N-heterocyclic carbene-palladium, ruthenium and iridium complexes were prepared with the racemic version of these new ligands by reacting the free NHCs with the appropriate metal precursors. The NHC-iridium complexes were then

View Article Online
DOI: 10.1039/C6DT04534K

transformed into their corresponding iridium-dicarbonyl species and used to analyse the electronic properties of the ligands. The incorporation of the 2-morpholinonaphthyl and 2-piperidinylnaphthyl groups had the effect of providing ligands of overall slightly more electronic-donating nature, with the piperidyl ligand showing TEP values normally found for alkyl-substituted NHC ligands (e.g. ICy).

Catalytic results with NHC-palladium and NHC-**GII** compounds were rather disappointing. The NHC-palladium complexes showed overall poor catalytic performance for this class of (pre)catalysts. When used as catalysts in Suzuki-Miyaura coupling reactions, they only provided good reactivity with the simplest chloro- and bromoarene substrates at room temperature. With the NHC-**GII** precatalysts as applied to representative ring-closing metathesis reactions of dienes and enynes, we only observed reasonable activity when running the reactions at elevated temperature (60°C) with toluene as the solvent. We believe that these results indicate that the second, hemilabile binding point of these ligands (morpholine, piperidine) is able to degrade the active catalyst species much more easily in the catalytic applications chosen here. The ligands we synthesised here should nevertheless prove useful in catalytic applications where such hemilability is essential for good catalytic activity and pertinent studies are underway in our laboratories.

4. Acknowledgements

AO thanks the Australian Government and UWA for a postgraduate scholarship. RD thanks the Australian Research council for funding (FT130101713). The Centre for Microscopy, Characterisation & Analysis at UWA is thanked for providing facilities and assistance.

5. Notes and references

1 J. E. Hill, T. A. Nile, *J. Organomet. Chem*., 1977, **137**, 293.
2 M. F. Lappert, R. K. Maskell, *J. Organomet. Chem*., 1984, **264**, 217.
3 A. J. Arduengo III, R.L. Harlow, M. J. Kline, *J. Am. Chem. Soc.,* 1991, **113**, 361.
4 W. A. Herrmann, M. Elison, J. Fischer, C. Kocher, G. R. J. Artus, *Angew. Chem. Int. Ed.,* 1995, **34***,* 2371.
5 T. Weskamp, W. C. Schattenmann, M. Spiegler, W. A. Herrmann, *Angew. Chem. Int. Ed.*, 1998, **37**, 2490.
6 M. Scholl, T. M. Trnka, J. P. Morgan, R. H. Grubbs, *Tetrahedron Lett*., 1999, **40**, 2247.
7 M. Scholl, S. Ding, C. W. Lee, R. H. Grubbs, *Org. Lett.,* 1999, **1**, 953.
8 J. Huang, E. D. Stevens, S. P Nolan, J. L Petersen, *J. Am. Chem. Soc*., 1999, **121**, 2674.
9 L. Ackermann, A. Fürstner, T. Weskamp, F. J. Kohl, W. A. Herrmann, *Tetrahedron Lett*., 2001, **40**, 4787.
10 For selected reviews on olefin metathesis see; a) G. C. Vougioukalakis, R. H. Grubbs, *Chem. Rev*., 2010, **110**, 1746. b) C. Samojłowicz, M. Bieniek, and K. Grela, *Chem. Rev*., 2009, **109**, 3708. c) Olefin Metathesis: Theory and Practice (Ed.: K. Grela), Wiley-VCH, Weinheim, **2014**.; d) S. Kress, S. Blechert, *Chem. Soc. Rev*., 2012, **41**, 4389.
11 K. Endo, R. H. Grubbs, *J. Am. Chem. Soc*., 2011, **133**, 8525.
12 E. M. Leitao, S. R. Dubberley, W. E. Piers, Q. Wu, R. McDonald, *Chem. Eur. J*., 2008, **14**, 11565.
13 M. S. Viciu, R. F. Germaneau, O. Navarro-Fernandez, E. D. Stevens, S. P. Nolan, *Organometallics*, 2002, **21**, 5470.
14 N. Marion, O. Navarro, J. Mei, E. D. Stevens, N. M. Scott, S. P. Nolan, *J. Am. Chem. Soc*., 2006, **128**, 4101.
15 M. G. Organ, S. Avola, I. Dubovyk, N. Hadei, E. A. B. Kantchev, C, J. O'Brien, C. Valente, *Chem. Eur. J.*, 2006, **12**, 4749.
16 G. Altenhoff, R. Goddard, C. W. Lehmann, F. Glorius, *J. Am. Chem. Soc.*, 2004, **126**, 15195.
17 S. Wuertz, C. Lohre, R. Froehlich, K. Bergander, F. Glorius, *J. Am. Chem. Soc.*, 2009, **131**, 8344.
18 a) X. Luan, R. Mariz, M. Gatti, C. Constabile, A. Poater, L. Cavallo, A. Linden, R. Dorta, *J. Am. Chem. Soc.*, 2008, **130**, 6848. b) L. Vieille-Petit, X. Luan, R. Mariz, S. Blumentritt, A. Linden, R. Dorta, *Eur. J. Inorg. Chem.*, 2009, 1861. c) L. Vieille-Petit, X. Luan, M. Gatti, S. Blumentritt, A. Linden, H. Clavier, S. P. Nolan, R. Dorta, *Chem. Commun.*, 2009, 3783. d) L. Vieille-Petit, H. Clavier, A. Linden, S. Blumentritt, S. P. Nolan, R. Dorta, *Organometallics*, 2010, **29**, 775. e) L. Wu, E. Drinkel, F. Gaggia, S. Capolicchio, A. Linden, L. Falivene, L. Cavallo, R. Dorta, *Chem. Eur. J.,* 2011, **17**, 12886. f) G. Sipos, A. Ou, B. W. Skelton, L. Falivene, L. Cavallo, R. Dorta, *Chem. Eur. J.*, 2016, **22**, 6939.
19 a) X. Luan, R. Mariz, C. Robert, M. Gatti, S. Blumentritt, A. Linden, R. Dorta, *Org. Lett.*, 2008, **10**, 5569.; b) X. Luan, L. Wu, E. Drinkel, R. Mariz, M. Gatti, R. Dorta, *Org. Lett.*, 2010, **12**, 1912.; c) L. Wu, L. Falivene, E. Drinkel, S. Grant, A. Linden, L. Cavallo, R. Dorta, *Angew. Chem. Int. Ed.*, 2012, **124**, 2924.
20 L. Wu, A. Salvador, A. Ou, M. W. Shi, B. W. Skelton, R. Dorta, *Synlett*, 2013, **24**, 1215.
21 Various chelating NHC structures that rely on the same design (additional ligation through the ortho position of aryl wingtips) have been successful, see: *N-Heterocyclic Carbenes* (Ed.: S. P. Nolan), Wiley-VCH: Weinheim, **2014**.
22 For representative examples: a) R. J. Lundgren, B. D. Peters, P. G. Alsabeh, M. Stradiotto, *Angew. Chem. Int. Ed*., 2010, **49**, 4071. b) R. J. Lundgren, M. Stradiotto, *Angew. Chem. Int. Ed*., 2010, ***49***, 8686. c) K. D. Hesp, R. J. Lundgren, M. Stradiotto, *J. Am. Chem. Soc*., 2011, **133**, 5194.
23 M. Gatti, L. Wu, E. Drinkel, F. Gaggia, S. Blumentritt, A. Linden, R. Dorta, *Arkivoc*, 2011, 176.
24 Crystallographic data for the structures reported in this paper have been deposited at the Cambridge Crystallographic Data Centre with supplementary publication numbers given below. Copies of the data can be obtained free of charge on application to CCDC, 12 Union Rd, Cambridge CB21EZ, UK (fax +441223336033; email deposit@ccdc.cam.ac.uk). Key details of the crystal and structure refinement data are summarized in the Supporting Information. CCDC files 1518956-1518966 contain crystallographic data for the crystal structures reported herein.
25 A. J. Arduengo III, R. Krafczyk, R. Schmutzler, H. A. Craig, A. Hugh, J. R. Goerlich, W. J. Marshall, M. Unverzagt, *Tetrahedron,* 1999**, 55**, 14523.
26 A. J. Arduengo III, J. R. Goerlich, W. J. Marshall, *J. Am. Chem. Soc.,* 1995**, 117***,* 11027.
27 M. K. Denk, A. Tadani, K. Hatano, A. Lough, *Angew. Chem. Int. Ed. Engl.,* 1997**, 36***,* 2607.
28 N. A. Giffin, A. D. Hendsbee, J. D. Masuda, *Acta Cryst.*, 2010, E**66**, o2194.
29 B. Su, R. Ganguly, Y. Li, R. Kinjo, *Angew. Chem. Int. Ed.*, 2014, **53**, 13106.
30 There is a minor signal (ca. 2%) showing at 9.22 ppm in the spectrum of **4c*** taken at -40°C. This is probably a tiny amount of starting material (**4c**) left in the mixture, although it might also be attributed to the *syn*-isomer of **4c***.

View Article Online
DOI: 10.1039/C6DT04534K

31 An alternative interpretation of the VT NMR spectra that does not involve ion pairing would be that splitting of the H_{im} signals is due to the generation of observable/frozen conformers within these *anti*-NHC salts as depicted below. The two sets of signals would then originate from the morpholyl/piperidyl groups approaching (set in red) or not (set in blue) the imidazolinium proton. Because VT NMR spectra of **4a** (see SI) or of any of our previously reported NHC salts without chiral counterion do not show any splitting of the *anti*-isomers, this alternative interpretation can be discarded.

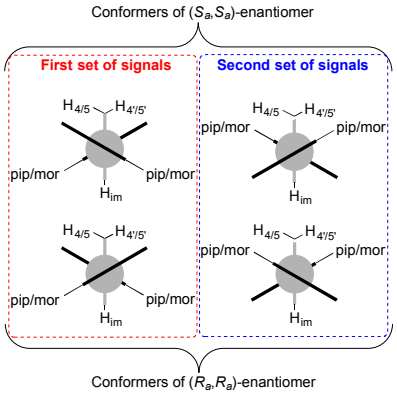

32 A. Chartoire, M. Lesieur, L. Falivene, A. M. Z. Slawin, L. Cavallo, C. S. J. Cazin, S. P. Nolan, *Chem. Eur. J.,* 2012, **18**, 4517.

33 For crystallographic data on **GII**, see: a) J. A. Love, M. S. Sanford, M. W. Day, R. H. Grubbs, *J. Am. Chem. Soc.*, 2003, **125**, 10103. b) S. E. Lehman, K. B. Wagener, *Organometallics,* 2005, **24**, 1477. c) C. Samojlowicz, M. Bieniek, A. Pazio, A. Makal, K. Wozniak, A. Poater, L. Cavallo, J. Wojcik, K. Zdanowski, K. Grela, *Chem. Eur. J.,* 2011, **17**, 12981.

34 a) R. A. Kelly III, H. Clavier, S. Giudice, N. M. Scott, E. D. Stevens, J. Bordner, I. Samardjiev, C. D. Hoff, L. Cavallo, S. P. Nolan, *Organometallics*, 2008, **27**, 202. b) D. J. Nelson, S. P. Nolan, *Chem. Soc. Rev.*, 2013, **42**, 6723.

35 For a first electronic evaluation of NHCs using such NHC-Ir complexes, see: a) A. R. Chianese, X. Li, M. C. Janzen, J. W. Faller, and R. H. Crabtree, *Organometallics,* 2003, **22**, 1663. For an early study on electronic changes induced by appropriate backbone substitution, see: b) D. M. Khramov, V. M. Lynch, C. W. Bielawski, *Organometallics*, 2007, **26**, 6042.

36 To understand if coordination of the morpholyl/piperidyl nitrogen is occurring in these NHC-Pd compounds, we attempted chloride abstraction with $AgPF_6$ on complex **6a**. Unfortunately, no clean complex could be isolated. See the Supporting Information for detail.

37 See ref 18c for time-conversion curves with (2-SICyNap)-**GII**. For time-conversion curves with **7a** and **7b**, please see the supporting information.

38 It is very difficult at this stage to understand why the RCM reactions in DCM do not work well with catalysts **7a** and **7b**. We would like to note that unsaturated metal complexes (such as **7a** and **7b**) can facilitate the Menshutkin reaction (nucleophilic substitution between a tertiary amine and an alkyl halide such as DCM) to such a point as to become problematic (see ref. 18f). While purely speculative, the tertiary amine incorporated in our ligand structures might start such a side reaction and ultimately impede catalysis in DCM.

TOC entry

Two new, potentially chelating NHC ligands are synthesised, characterised and their preliminary catalytic activity in NHC-Pd and NHC-Ru complexes is evaluated.